

NWRI GRADUATE FELLOW PROGRESS REPORT

DATE: July 25th, 2025

Project Title: Phosphate recovery from municipal wastewater using reverse-selective ion exchange membrane

Full Name: Xinyi Wang Advisor: David Jassby

Institution: University of California, Los Angeles

Background and Introduction

Overview

Phosphate is an irreplaceable element in fertilizer formulations crucial for enhancing crop yields, with global demand exceeding 30 million metric tons annually. (Matsubae et al., 2015; Petzet & Cornel, 2011) Recognizing wastewater as a phosphate-rich resource, conventional wastewater treatment plants have traditionally relied on settlement, adsorption, chemical precipitation, and biological sequestration to mitigate phosphate levels in treated wastewater and prevent eutrophication in receiving water bodies.(Finnerty et al., 2024; Loganathan et al., 2014; Tarayre et al., 2016; Ye et al., 2017, 2018) Efforts toward phosphate recovery from wastewater have gained momentum, with chemical adsorption and precipitation methods widely explored.(Ahmed & Tewari, 2018; Kumar & Pal, 2015; Nieminen, n.d.)

Selective phosphate recovery has emerged as a promising alternative, with mixed-matrix membranes garnering attention in resource extraction applications owing to their capacity for chemical-free, low-energy operation and waste minimization. (Bernardo & Drioli, 2017; Buonomenna & Bae, n.d.; Zuo et al., 2021) Pioneering work by Iddya et al. (2022) proposed a novel strategy for selective phosphate recovery through the fabrication of reverse-selective ion exchange membranes. The paper highlighted the dependency of phosphate flux on HMO loading, which was largely dependent on the ionic exchange capacity (IEC) of the membrane, as the initial step in HMO growth involved the impregnation of the cation exchange membrane (CEM) with Mn⁴⁺ ions. Due to this limitation, a mass loading of 11% was the maximum achievable value. (Iddya et al., 2022) The primary objective of this project is to innovate the mixed matrix membrane fabrication and enhance the phosphate flux. Secondly, we will integrate this advanced membrane in our pilot resource recovery system. This project aims to establish a paradigm shift in wastewater treatment methodologies, laying the groundwork for sustainable resource utilization and environmental stewardship.

By pioneering this innovative approach, we anticipate significant advancements in the fields of membrane technology and wastewater treatment, with far-reaching implications for sustainability and resource management.

Hypothesis

In this research, we hypothesize that by synthesizing HMO nanoparticles separately and blending them into a cation exchange polymer matrix, we can achieve a higher HMO loading than is possible through in-membrane growth. This enhanced loading is expected to significantly increase phosphate flux and improve overall membrane performance.

Study Goals

The primary goals of this research are to increase the phosphate flux of the membrane by at least fivefold while achieving a selectivity for phosphate over competing ions that is at least tenfold. In addition, we aim to fabricate a larger-sized membrane suitable for pilot-scale testing and potential real-world application.

• Objectives of Research Project

- · Synthesize HMO nanoparticles with controlled size and morphology.
- Fabricate dense ion-exchange membranes with a relatively high IEC.
- · Achieve homogeneous dispersion of nanoparticles within the cation-exchange polymer matrix.
- · Conduct comprehensive membrane characterization, performance testing, and iterative optimization.
- · Scale up to fabricate and test larger mixed-matrix membranes for pilot-scale evaluation.

Need(s) Served by This Research

This research addresses the need for more efficient and selective membranes for nutrient recovery in wastewater treatment. By advancing mixed-matrix membrane technology, we aim to significantly enhance resource recovery, making wastewater treatment processes not only more sustainable but potentially profitable by reclaiming valuable constituents such as phosphate. Moreover, the findings will lay a foundation for broader applications of MMMs in targeted extraction, contributing to both environmental protection and circular resource management.

Progress to Date

HMO nanoparticle synthesis

Amorphous HMO particles were synthesized following the previously reported method. (Parida et al., 1981) In short, 40 g KMnO₄ was dissolved in 500 ml Milli-Q water, with the pH adjusted to 12.5 using 1 M NaOH. Subsequently, the KMnO₄ solution was slowly added dropwise into an equal volume containing 60 g MnSO₄·H₂O under vigorous stirring. This process led to the formation of HMO particles, which were then recovered by filtration using a vacuum filter. The obtained HMO particles were washed with Milli-Q water until the pH of the wash water reached 7. The washed HMO was subsequently placed in a petri dish and dried in an oven at 50 °C for 72 hours. Following drying, the HMO particles were ground and stored in a glass bottle within a vacuum desiccator for further use. A diagram describing the HMO particles synthesis process can be found in Figure 1.

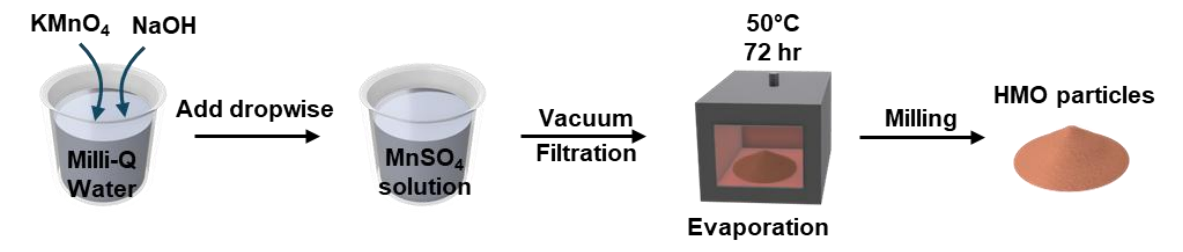


Figure 1. Diagram of HMO particle synthesis.

• Membrane fabrications

The membrane was fabricated by evaporation, followed by thermal annealing treatment. The pure SPES membrane and HMO particles-loaded membrane were fabricated following the same procedure. The pure SPES membrane was denoted as MEO. HMO particle loading was calculated using equation (1), where $w_{HMO}\%$ represents the HMO nanoparticle loading, m_{HMO} (g) is the mass of the HMO nanoparticles, m_{SPES} (g) is the mass

of the SPES polymer. 20wt% and 40wt% HMO-loaded polymer solutions were prepared and used for membrane fabrication; the membranes were denoted as ME20 and ME40, respectively. Pure SPES membranes and 40 wt% HMO loading membranes without thermal annealing were prepared and labeled as ME0 NTA and ME40 NTA, respectively, to serve as control experiments for thermal annealing.

$$w_{HMO}\% = \frac{m_{HMO}}{m_{HMO} + m_{SPES}} \times 100$$
 (1)

An SPES solution was prepared by dissolving 30 g SPES in 70 g NMP. The SPES was added gradually at a rate of 5 g·hr⁻¹ while heating at 60 °C and stirring. The solution was stirred for 24 hours at 250 RPM and 60 °C. Subsequently, the solution was cooled to room temperature and covered with a porous lid for 5 hours for degassing in a vacuum desiccator. The SPES solution was then stored at room temperature in a vacuum desiccator until further use.

For the HMO-SPES solution, 7.5 and 20 grams of HMO nanoparticles were suspended in 70 g NMP and stirred for 30 min for 20 wt% HMO loading and 40wt% HMO loading, respectively. After that, 30 g of SPES solution was added gradually at a rate of 5 g·hr⁻¹ under heating at 60 °C and stirring at 250 RPM for 24 hours. The solution was then cooled down to room temperature and covered with a porous lid for 5 hours for degassing in a vacuum desiccator. The HMO-SPES solution was stored at room temperature in a vacuum desiccator until further use.

Next, 15 g polymer/particle solution was poured onto a glass plate, and a casting knife with a 400 μ m blade height was used to cast the membrane. The plate was transferred to a vacuum oven (Across International LLC, New Jersey, U.S.A) set to 50 °C, and the temperature was gradually increased to 100 °C (1 °C.min⁻¹), once the vacuum pressure reached -580 mm Hg. The membrane was kept in the vacuum oven at 100 °C for 24 hours before reducing the temperature to 50 °C (-0.3 °C.min⁻¹) and venting. After transferring the plate to a Milli-Q water bath for 30 minutes, the membrane detached and floated to the surface. It was then placed on a clean, dry glass plate wrapped in aluminum foil and transferred back to the vacuum oven at 50 °C. Once the vacuum pressure reached -580 mm Hg, the temperature was increased to 140 °C (1 °C.min⁻¹) and maintained for 1 hour for thermal annealing. Finally, the membrane was removed from the oven and stored in a 0.5 M NaH₂PO₄·H₂O solution until use. A diagram describing the membrane fabrication is shown in Figure 2.

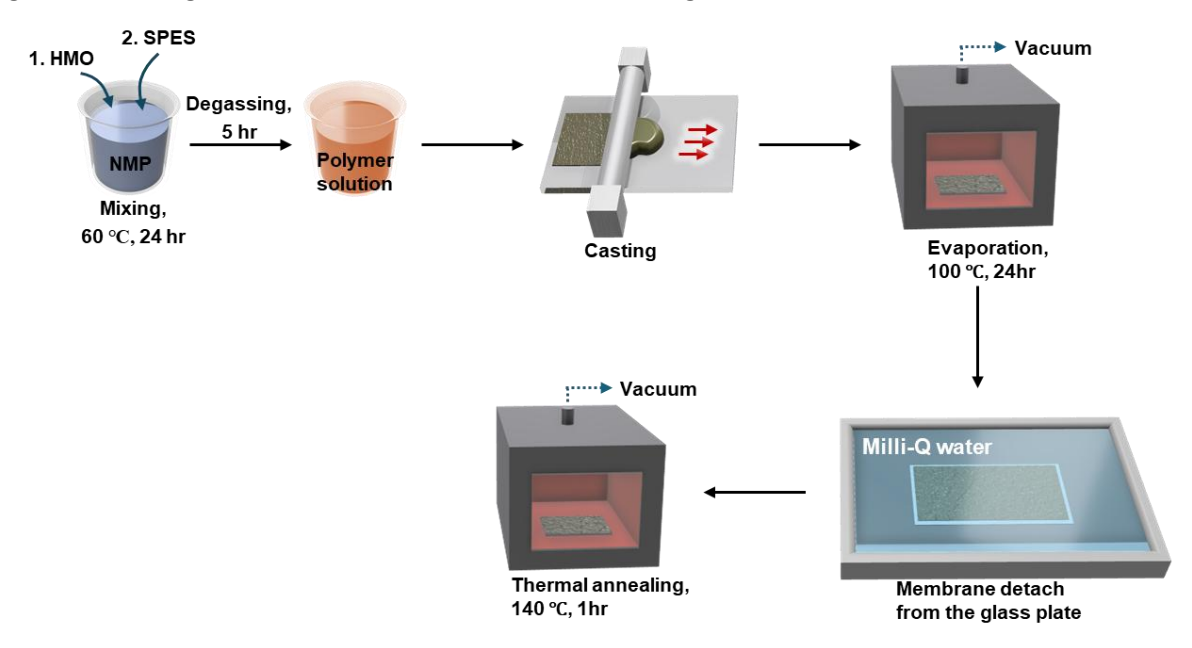


Figure 2. Diagram of membrane fabrication.

Membrane testing condition and setup

The membrane was tested in a diffusion cell (Figure 3a). Membranes were evaluated over a 24-hour period, during which continuous stirring was maintained in both the feed and receiving chambers. For the phosphate flux test, a feed solution comprising 0.1 M NaH₂PO₄·H₂O was employed, while the permeate solution consisted of 0.05 M Na₂SO₄. In the membrane selectivity tests, the feed solution contained equimolar concentrations (0.01 M) of NaCl, NaH₂PO₄·H₂O, Na₂SO₄, and NaNO₃, whereas Milli-Q water served as the permeate solution for the receiving chamber. Municipal wastewater has an average pH of 6.2 ± 0.1, where phosphate is predominantly in the form of H₂PO₄⁻. (Han, 2020; Pedrouso et al., 2021)Throughout the experiment, the pH of both the feed and permeate solutions was maintained below 6 to ensure this phosphate speciation. During testing, the pH of the solution was monitored using a pH probe (Orion Star A121, Thermo Fisher Scientific, Inc., Waltham, MA, USA) and pH meter (Orion Star A221 Portable pH Meter, Thermo Fisher Scientific, Inc., Waltham, MA, USA). Phosphate concentrations were determined using HACH vial tests (TNT 844, TNT843, HACH, Loveland, CO, USA) and a HACH spectrophotometer (HACH DR1900, Loveland, CO, USA), while nitrate concentrations were measured via total nitrogen (TN) analysis (TOC-L CSN, Shimadzu Co., Kyoto, Japan). Chloride concentration was assessed using a pH/conductivity meter (ORION STAR A215, Thermo Fisher Scientific, Inc., Waltham, MA, USA) and a chloride probe (Thermo Scientific, Chloride electrode 9417BN, Waltham, MA, USA), and sulfur concentration was determined using Inductively Coupled Plasma Mass Spectrometry (ICP-MS, Shimadzu, Japan).

Ion flux calculations were performed using equation (2), where J_{-} (mmol.m⁻².hr⁻¹) represents the ion flux, "_" can be phosphate (J_P) , sulfate (J_S) , nitrate (J_N) , or chloride (J_{Cl}) flux. $C_{-}(ppm)$ represents the ion concentrations in the receiving chamber after the experiment, "_" can be phosphate, sulfate, nitrate or chloride concentration, $V_R(L)$ signifies the volume of water in the receiving chamber at the end of the experiment. mw_{-} (mg/mmol) represents the molecular weight of the ion of interest. A_m (m²) denotes the membrane area, and 24 (hr) denotes the duration of the experiment. Membrane selectivity was determined using equation (3), where $S_{P/_{-}}$ represents the selectivity of phosphate over other ions (nitrate, chloride, or sulfate). J_P (mmol.m⁻².hr⁻¹) is the phosphate flux, and J (mmol.m⁻².hr⁻¹) denotes the flux of sulfate, nitrate, or chloride.

$$J_{-} = \frac{C_{-} \times V_{R}}{mw_{-} \times A_{m} \times 24}$$

$$S_{P/_{-}} = \frac{J_{P}}{I}$$
(3)

Phosphate flux test:

Feed: 150 g 0.1 M NaH₂PO₄·H₂O, pH 4.59 Receiving: 150 g 0.05 M Na₂SO₄, pH 6.24

Duration: 24 hr Selectivity test:

Feed: 150 g 0.01 equimolar NaH₂PO₄·H₂O, NaCl, NaNO₃, Na₂SO₄, pH 4.93

Receiving: 150 g Milli-Q water, pH 6.72

Duration: 24 hr

Results and discussion

Membranes with varying HMO loadings (with and without thermal annealing) were assessed for phosphate flux and selectivity (Figures 3b-d). Phosphate flux measurements show that as the HMO loading increased, there was a corresponding increase in phosphate flux (ME40 > ME20 > ME0) (Figure 3b). Specifically, at the highest mass loading (ME40), the phosphate flux was 13X larger compared to the control with no HMO particles (ME0) (Figure

3b), and was 20X larger compared to a commercial CEM (0.077 ± 0.004 mmol.m⁻².h⁻¹). However, it is worth noting that the loading of HMO cannot be infinitely increased due to compatibility concerns between HMO and SPES polymer, particle leaching at high mass loading, and overall material brittleness.(Xu et al., 2018) Membranes that were not thermally annealed (ME40 NTA) exhibited the highest phosphate flux, but showed poor selectivity (Figure 3c, d). This is likely because of the porous nature of the non-thermally annealed materials. Phosphate flux through a commercial anion exchange membrane (AEM) was evaluated by others, and found to be significantly impacted by competing ion concentrations. (McCartney et al., 2022) In general, phosphate fluxes through AEMs were found to range between 3 mmol.m⁻².h⁻¹ to 100 mmol.m⁻².h⁻¹depending on the composition of the solution under diffusion dialysis conditions. Critically, AEMs show little selectivity towards phosphate. (McCartney et al., 2022)

Selectivity values were plotted on a logarithmic scale (Figure 3d), with values below 1 indicating lower phosphate flux compared to competing ions. ME40 exhibited the highest selectivity for phosphate over nitrate and chloride $(11.34 \pm 0.49 \text{ and } 8.79 \pm 0.09 \text{ over nitrate and chloride, respectively})$ with selectivity for sulfate > 104, as sulfate concentrations were below the ICP-MS detection limit (0.04 ppm). The extremely low concentration of sulfate can be attributed to its divalent charge, leading to stronger electrostatic repulsion between the SPES and sulfate, resulting in a lower Donnan potential. (Donnan, 1924; Pakizeh et al., 2020) The selectivity towards chloride and nitrate can also be explained by the Donnan repulsion between these anions and the negative sulfonate groups on the SPES polymer. In contrast, phosphate ions can form specific outer-sphere interactions with the embedded HMO particles, which allows these ions to move across the membrane, and results in the observed selectivity towards phosphate. Individual ion flux measurements in the thermally annealed membranes show that increasing HMO loading into the membranes resulted in increased phosphate fluxes while competing anions showed no significant change in flux (Figure 3c). This is likely because of the good compatibility of the HMO particles with the SPES polymer, which leads to a defect-free structure that allows for phosphate "hopping" across the HMO particles while prohibiting other anion transport across the polymer. (Iddya et al., 2022; Karmakar et al., 2017)The non-thermally annealed materials showed poor selectivity towards chloride and nitrate, but good selectivity towards sulfate (Figure 3c,d). In terms of individual ion fluxes, all anions showed higher fluxes compared to the thermally annealed membranes (Figure 3c). Again, it is probable that the porous structure of the non-thermally annealed materials led to less selective pathways through the membrane material. However, it is possible that the divalent charge of sulfate ions still allowed the non-thermally annealed membrane to reject this species. (Geise et al., 2013; Park et al., 2017; Restrepo-Flórez & Maldovan, 2019)

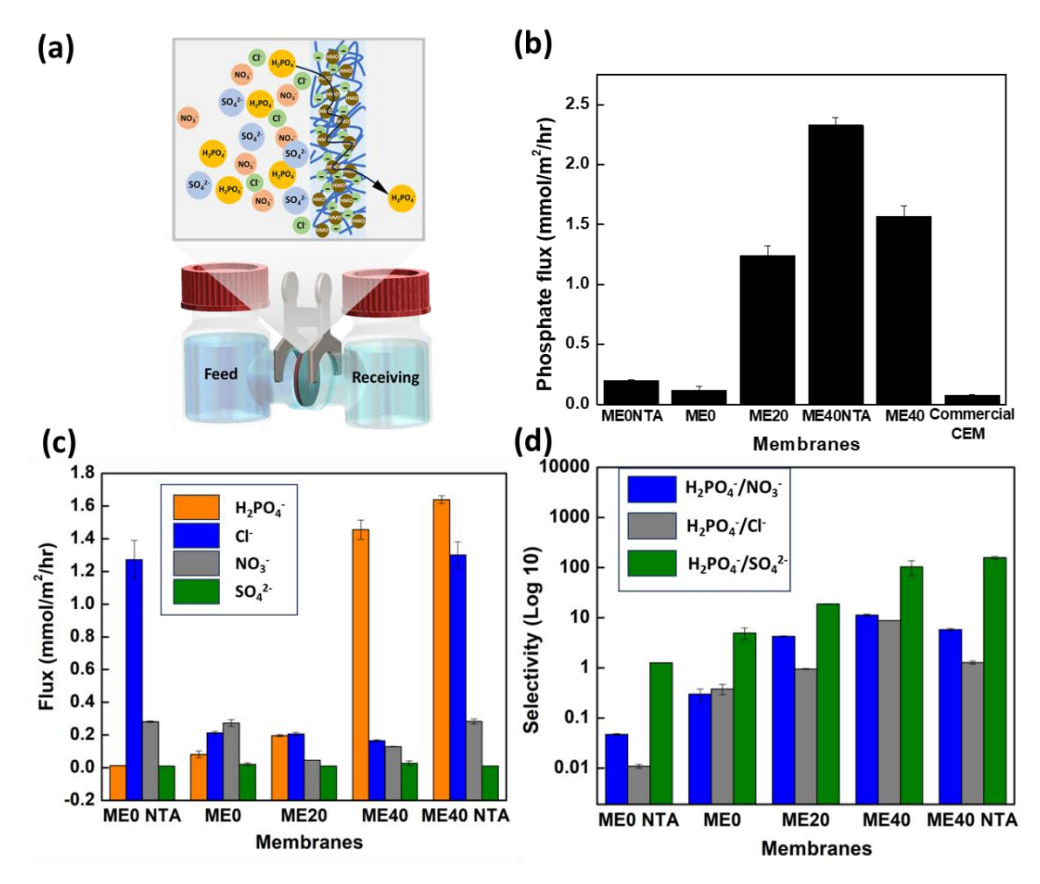


Figure 3 (a) Experimental setup, (b) Phosphate flux result for membranes tested in 0.1 M NaH₂PO₄·H₂O feed solution, (c) Ion fluxes for membranes tested in 0.01 equimolar NaH₂PO₄·H₂O, NaCl, NaNO₃, and Na₂SO₄. (d) Selectivity of phosphate over competitive ions on a log scale,

Conclusions

We successfully embedded pre-formed HMO nanoparticles within a SPES-based cation exchange membrane, thereby enhancing phosphate flux by a factor of 8.5 over our previously published results (Iddya et al., 2022). Membranes were formed by a typical EvIPS process followed by annealing at high temperatures. The best-performing membrane – denoted as ME40 herein – exhibited a phosphate flux of 1.57 mmol.m⁻².h⁻¹ and selectivity of 9, 11, and 104 over chloride, nitrate, and sulfate, respectively. Our findings highlight the necessity of thermal annealing treatment for optimal phosphate selectivity; also, we determined that a loading of 28 wt% is the maximum feasible without compromising MMM mechanical properties. These results signify a significant advancement in the application of MMMs for phosphate extraction from wastewater, thereby opening new avenues for sustainable water treatment technologies.

Next Steps

While the membrane demonstrated promising performance at the lab scale, scaling up remains challenging. At higher HMO loading rates, the membrane becomes brittle, making it difficult to fabricate larger sheets without cracking—particularly at 40 wt% HMO, where some membranes fractured during the evaporation process. This limitation currently prevents straightforward application in pilot testing and real-world scenarios.

In the next phase, we will investigate the underlying mechanisms governing the interactions among the polymer, nanoparticles, solvent, and nonsolvent to understand how each component influences membrane morphology and mechanical properties. Guided by these insights, we will optimize the formulation by selecting suitable solvent

and nonsolvent systems to improve flexibility and integrity at high HMO loading. We plan to fabricate new phosphate-recovery membranes, characterize them using SEM imaging, and evaluate their selectivity, phosphate transport efficiency, and tensile strength. These studies will not only address the brittleness challenge but may also open additional questions regarding the trade-off between loading content, mechanical durability, and recovery performance, which we will explore through iterative testing.

References

- Ahmed, A., & Tewari, S. (2018). Capacitive deionization: Processes, materials and state of the technology. *Journal of Electroanalytical Chemistry*, 813(February), 178–192.
- Bernardo, P., & Drioli, E. (2017). 4.9 Membrane Technology in the Refinery and Petrochemical Field: Research Trends and Recent Progresses. *Comprehensive Membrane Science and Engineering*, 164–188.
- Buonomenna, M. G., & Bae, J. (n.d.). *Membrane processes and renewable energies*. Donnan, F. G. (1924). The theory of membrane equilibria. *Chemical Reviews*, 1(1), 73–90.
- Finnerty, C. T. K., Childress, A. E., Hardy, K. M., Hoek, E. M. V., Mauter, M. S., Plumlee, M. H., Rose, J. B., Sobsey, M. D., Westerhoff, P., Alvarez, P. J. J., & Elimelech, M. (2024). The Future of Municipal Wastewater Reuse Concentrate Management: Drivers, Challenges, and Opportunities. *Environmental Science and Technology*,
- Geise, G. M., Hickner, M. A., & Logan, B. E. (2013). Ionic resistance and permselectivity tradeoffs in anion exchange membranes. *ACS Applied Materials and Interfaces*, *5*(20), 10294–10301.
- Han, K. N. (2020). Characteristics of precipitation of rare earth elements with various precipitants. *Minerals*, 10(2).
- Iddya, A., Zarzycki, P., Kingsbury, R., Khor, C. M., Ma, S., Wang, J., Wheeldon, I., Ren, Z. J., Hoek, E. M. V., & Jassby, D. (2022). A reverse-selective ion exchange membrane for the selective transport of phosphates via an outer-sphere complexation—diffusion pathway. *Nature Nanotechnology*, *17*(11), 1222–1228.
- Karmakar, S., Bhattacharjee, S., & De, S. (2017). Experimental and modeling of fluoride removal using aluminum fumarate (AlFu) metal organic framework incorporated cellulose acetate phthalate mixed matrix membrane.
- Kumar, R., & Pal, P. (2015). Assessing the feasibility of N and P recovery by struvite precipitation from nutrient-rich wastewater: a review. *Environmental Science and Pollution Research*, 22(22), 17453–17464.
- Loganathan, P., Vigneswaran, S., Kandasamy, J., & Bolan, N. S. (2014). Removal and recovery of phosphate from water using sorption. *Critical Reviews in Environmental Science and Technology*, 44(8), 847–907.
- Matsubae, K., Yamasue, E., Inazumi, T., Webeck, E., Miki, T., & Nagasaka, T. (2015). *Innovations in steelmaking technology and hidden phosphorus flows*.
- McCartney, S. N., Fan, H., Watanabe, N. S., Huang, Y., & Yip, N. Y. (2022). Donnan dialysis for phosphate recovery from diverted urine. *Water Research*, 226, 119302.
- Nieminen, J. (n.d.). PHOSPHORUS RECOVERY AND RECYCLING FROM MUNICIPAL WASTEWATER SLUDGE.
- Pakizeh, M., May, P., Matthias, M., & Ulbricht, M. (2020). Preparation and characterization of polyzwitterionic hydrogel coated polyamide-based mixed matrix membrane for heavy metal ions removal. *Journal of Applied Polymer Science*, 137(48).
- Parida, K. M., Kanungo, S. B., & Sant, B. R. (1981). Studies on MnO2—I. Chemical composition, microstructure and other characteristics of some synthetic MnO2 of various crystalline modifications. *Electrochimica Acta*, 26(3), 435–443.

- Park, H. B., Kamcev, J., Robeson, L. M., Elimelech, M., & Freeman, B. D. (2017). Maximizing the right stuff: The trade-off between membrane permeability and selectivity. *Science*, *356*(6343), 1138–1148.
- Pedrouso, A., Val del Rio, A., Morales, N., Vazquez-Padin, J. R., Campos, J. L., & Mosquera-Corral, A. (2021). Mainstream anammox reactor performance treating municipal wastewater and batch study of temperature, pH and organic matter concentration cross-effects. *Process Safety and Environmental Protection*, 145, 195–202.
- Petzet, S., & Cornel, P. (2011). Towards a complete recycling of phosphorus in wastewater treatment-options in Germany.
- Restrepo-Flórez, J. M., & Maldovan, M. (2019). Permeabilities and selectivities in anisotropic planar membranes for gas separations. *Separation and Purification Technology*, 228, 115762.
- Tarayre, C., De Clercq, L., Charlier, R., Michels, E., Meers, E., Camargo-Valero, M., & Delvigne, F. (2016). New perspectives for the design of sustainable bioprocesses for phosphorus recovery from waste. *Bioresource Technology*, 206, 264–274.
- Xu, R., Wang, Z., Wang, M., Qiao, Z., & Wang, J. (2018). High nanoparticles loadings mixed matrix membranes via chemical bridging-crosslinking for CO 2 separation.
- Ye, Y., Hao Ngo, H., Guo, W., Liu, Y., Li, J., Liu, Y., Zhang, X., Jia, H., Barcelo, D., & Ngo, H. H. (2017). Insight into chemical phosphate recovery from municipal wastewater. *Science of the Total Environment*, *576*, 159–171.
- Ye, Y., Ngo, H. H., Guo, W., Liu, Y., Chang, S. W., Nguyen, D. D., Liang, H., & Wang, J. (2018). A critical review on ammonium recovery from wastewater for sustainable wastewater management. In *Bioresource Technology* (Vol. 268, pp. 749–758). Elsevier Ltd.
- Zuo, K., Wang, K., DuChanois, R. M., Fang, Q., Deemer, E. M., Huang, X., Xin, R., Said, I. A., He, Z., Feng, Y., Shane Walker, W., Lou, J., Elimelech, M., Huang, X., & Li, Q. (2021). Selective membranes in water and wastewater treatment: Role of advanced materials. *Materials Today*, *50*, 516–532.